Automatic Segmentation of Vessels in In-Vivo Ultrasound Scans

Tamimi-Sarnikowski, Philip; Brink-Kjær, Andreas; Moshavegh, Ramin; Jensen, Jørgen Arendt

Published in:
Proceedings of SPIE

Link to article, DOI:
10.1117/12.2254101

Publication date:
2017

Document Version
Publisher's PDF, also known as Version of record

Automatic Segmentation of Vessels in In-Vivo Ultrasound Scans

Philip Tamimi-Sarnikowski, Andreas Brink-Kjær, Ramin Moshavegh, and Jørgen Arendt Jensen

Center for Fast Ultrasound Imaging, Dept. of Elec. Eng., Technical University of Denmark, DK-2800 Lyngby, Denmark

ABSTRACT

Ultrasound has become highly popular to monitor atherosclerosis, by scanning the carotid artery. The screening involves measuring the thickness of the vessel wall and diameter of the lumen. An automatic segmentation of the vessel lumen, can enable the determination of lumen diameter. This paper presents a fully automatic segmentation algorithm, for robustly segmenting the vessel lumen in longitudinal B-mode ultrasound images. The automatic segmentation is performed using a combination of B-mode and power Doppler images. The proposed algorithm includes a series of preprocessing steps, and performs a vessel segmentation by use of the marker-controlled watershed transform. The ultrasound images used in the study were acquired using the bk3000 ultrasound scanner (BK Ultrasound, Herlev, Denmark) with two transducers "8L2 Linear" and "10L2w Wide Linear" (BK Ultrasound, Herlev, Denmark). The algorithm was evaluated empirically and applied to a dataset of in-vivo 1770 images recorded from 8 healthy subjects. The segmentation results were compared to manual delineation performed by two experienced users. The results showed a sensitivity and specificity of 90.41 ± 11.2 % and 97.93 ± 5.7 % (mean $\pm$ standard deviation), respectively. The amount of overlap of segmentation and manual segmentation, was measured by the Dice similarity coefficient, which was 91.25 ± 11.6 %. The empirical results demonstrated the feasibility of segmenting the vessel lumen in ultrasound scans using a fully automatic algorithm.

Keywords: Automatic segmentation, ultrasound imaging, watershed transform, vascular disease

1. INTRODUCTION

Cardiovascular disease (CVD) is one of the main causes of death worldwide. CVD is typically associated with atherosclerosis, which is the thickening/degeneration of vessel walls.[1] B-mode ultrasound images are widely used in clinical practice to monitor atherosclerotic progression. Early detection of atherosclerosis enables prophylactic treatment, which reduces the risk of developing serious injuries.[2,1] Clinical screening procedures for atherosclerosis, involve scanning of the common carotid artery (CCA). Two of the primary screening variables are the diameter of the CCA lumen and the intimia-media thickness (IMT).[3] These have created the motivation for developing semi- and fully automatic methods for segmenting the vessel lumen. This paper presents a novel approach for automatic segmentation of the vessel lumen, based on the marker-controlled watershed transform.[4] The segmentation of vessels is an already established field. Existing methods are based on B-mode ultrasound scans alone,[5,6] or in combination with contrast-enhanced ultrasound images.[7] The novel method proposed in this article uses a combination of B-mode ultrasound images, and flow information in the form of power Doppler images. The remainder of this paper is organized as follows. Section 2 describes the proposed algorithm. Section 3 presents the in-vivo results with a following discussion. Section 4 concludes the paper and provides perspective for the future work.

Further author information: Philip Tamimi-Sarnikowski, E-mail: p.sarnikowski@gmail.com
Andreas Brink-Kjær, E-mail: andreas-bk@live.dk

Medical Imaging 2017: Biomedical Applications in Molecular, Structural, and Functional Imaging
edited by Andrzej Krol, Barjor Gimi, Proc. of SPIE Vol. 10137, 101371P · © 2017 SPIE
CCC code: 1605-7422/17/$18 · doi: 10.1117/12.2254101

2. MATERIALS AND METHODS

The purpose of the proposed algorithm is to segment the vessel lumen in ultrasound images using both B-mode and power Doppler images. The underlying segmentation method of the proposed algorithm is the marker-controlled watershed transform.[4] The algorithm can be divided into four distinct steps, which are explained in this section. The first step is a pre-processing step in which the image is cropped to the region of interest, speckle noise is decreased and contrast between the vessel lumen and walls is increased. The second step creates a set of markers from which the watershed transform is initiated. The third step computes the marker-controlled watershed transform. The last step selects and refines regions associated with the vessel lumen. The steps will be illustrated using two different views, namely the CCA and the femoral artery bifurcation (FAB).

2.1 Step 1. Preprocessing of B-mode image

The preprocessing of the B-mode image has three objectives: to crop the image, decrease speckle noise, and enhance the vessel boundary. The image is cropped to remove dark shadow regions, thereby reducing the computational load.[5] The image is binarized using a morphological opening followed by an intensity threshold, which can be seen in Fig. 1b. The position of the first and last white pixel is found, along the lateral and axial axis. The image is cropped using these pixel indices as seen in (Fig. 1c).

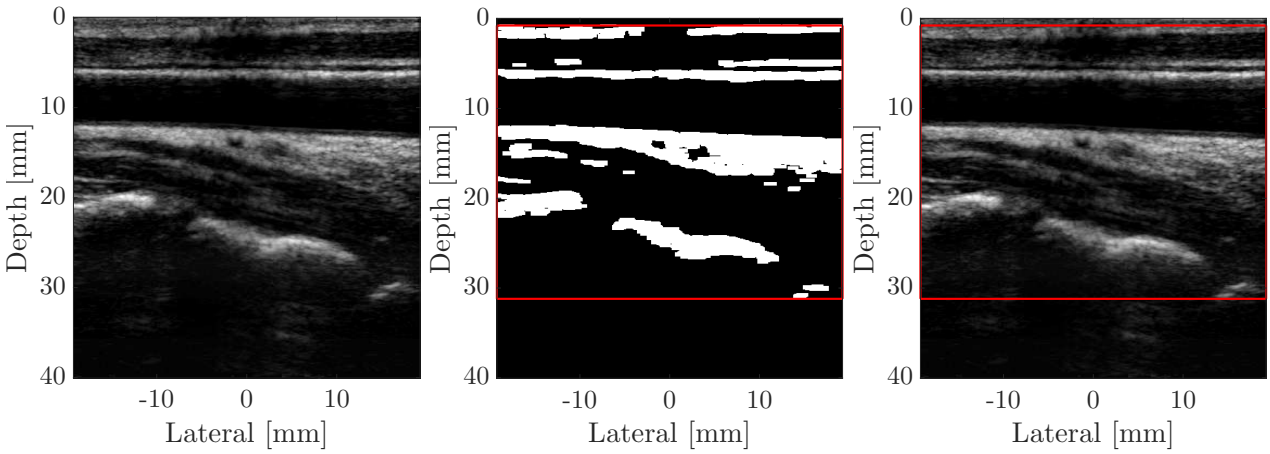

Figure 1: Illustration of image cropping process. The image is cropped to 76% of the original size. **(a)** Original B-mode image. **(b)** Binarized B-mode image, with cropping border in red. **(c)** B-mode image with cropping border superimposed.

The images presented throughout the rest of the article are cropped according to the illustrated process above. The B-mode image is filtered with a 2-D Wiener filter[8] to remove speckle noise and avoid over-segmentation. The 2-D wiener filter is an adaptive noise removal filter, which estimates the noise in the image, by use of local neighborhood statistics. The vessel boundaries are highlighted to increase the contrast between vessel lumen and vessel wall. This is achieved with morphologic reconstruction by opening and closing.[9]

The brightest interface encountered in vessel images is usually between the vessel wall and the vessel lumen, since this is where the largest change in acoustic impedance occurs. In some cases, parts of the vessel wall will not be visible, because of angle dependency. The proposed algorithm uses an edge connecting method to resolve this issue. The edges in the images are found initially using a canny filter.[10] These edges are connected using two constraints. Firstly, the euclidean pixel distance between the end points should be less than a threshold, which is based on the image size. Secondly, the orientation of the edges should not be the same. The connected edges are then enlarged using morphological dilation. The edges are added to the morphologically reconstructed B-mode images (see Fig. 2).

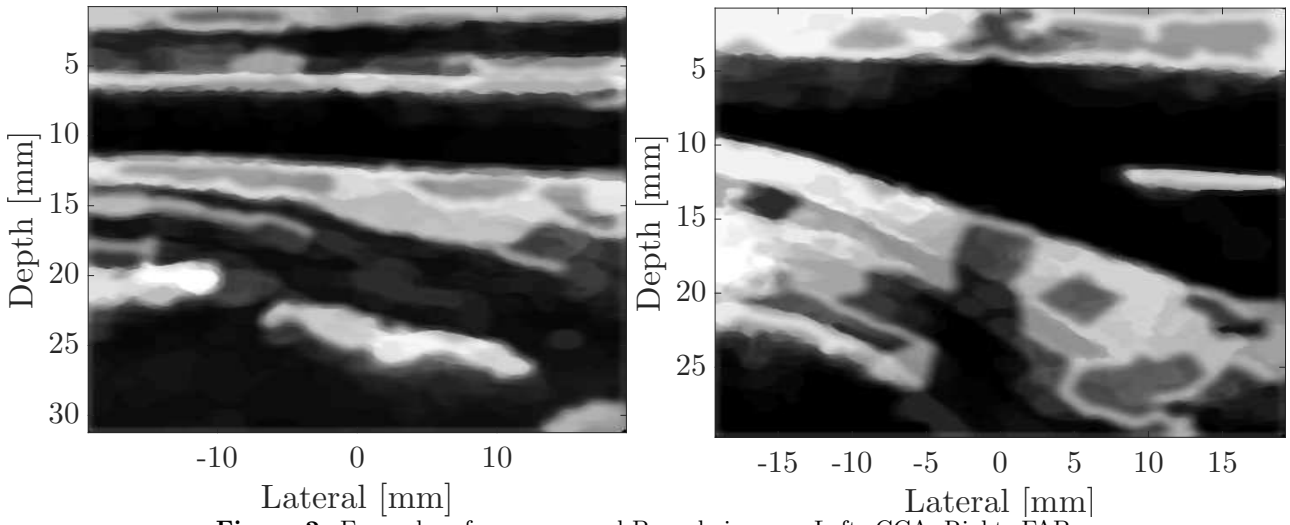

Figure 2: Examples of pre-processed B-mode images. Left: CCA. Right: FAB.

2.2 Step 2. Generation of markers

Beucher[4] showed that initiating the watershed transform from a predefined set of markers, highly reduces the computational load and over-segmentation in gradient images. The proposed algorithm generates a marker image, consisting of two sets of markers, one set within the vessel lumen, and the other in the neighboring tissue. The inner and outer markers enables the marker-controlled watershed to separate the vessel lumen from surrounding tissue. The flow information from the power Doppler images are used to generate the inner markers. A total of 81 frames of the power Doppler images, containing at least one cardiac cycle, are averaged for every B-mode image to compensate for the pulsating flow (see Fig. 3a). The inner markers are generated by computing the center-line of the averaged power Doppler images. Calculating the center-line is the process of thinning out a binary image to a spine of a one pixel width.

The outer markers are generated by thresholding the B-mode image, to select pixels with high intensity, producing a binary image. Following this, the binary image is multiplied with the inverse power Doppler image to remove outer markers within the vessel lumen. The complete marker images are shown in Fig. 3b with the inner and outer markers in orange and blue colors, respectively.

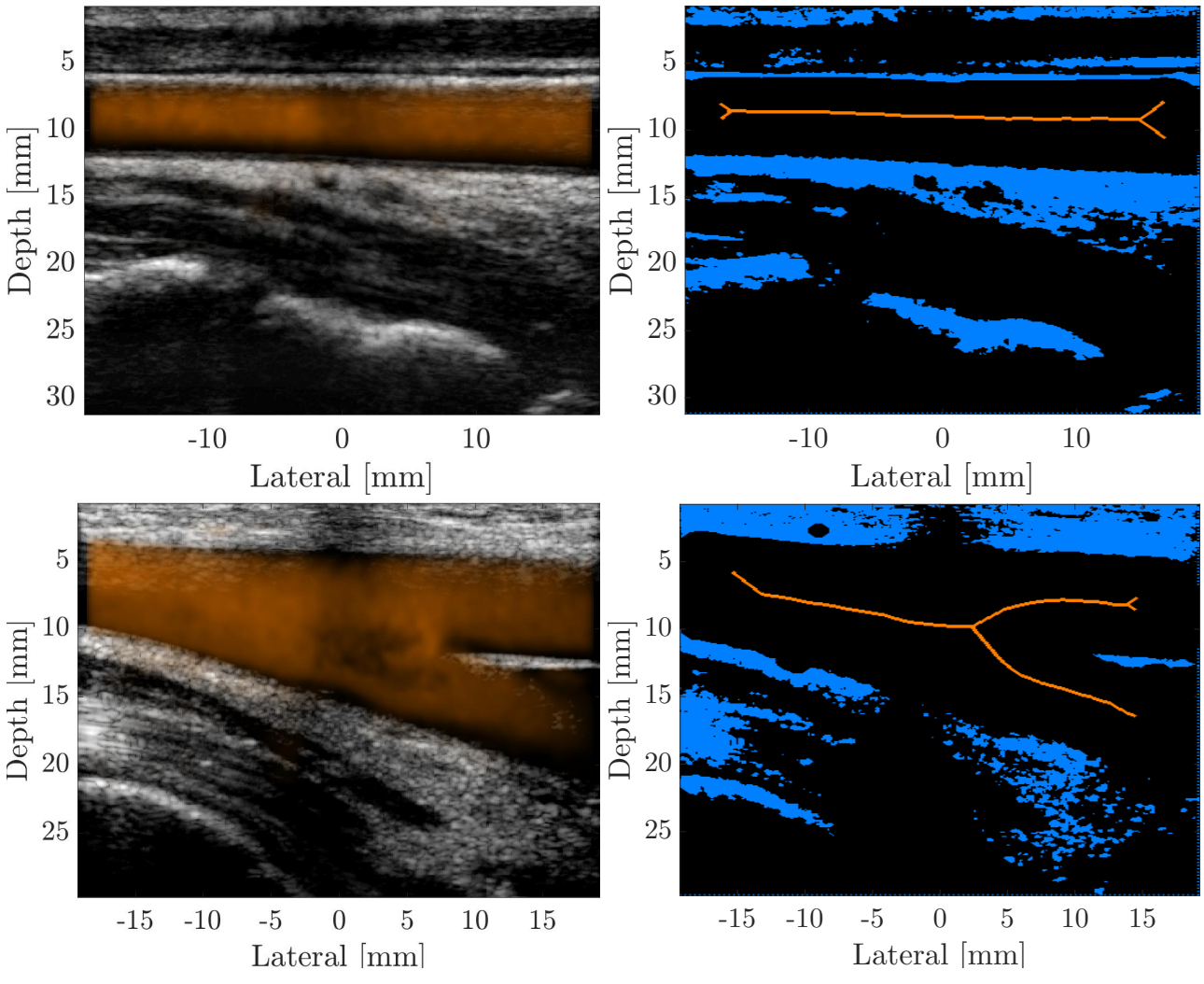

Figure 3: Examples of marker images. Top: CCA. Bottom: FAB. **(a)** Average of 81 power Doppler images superimposed on the B-mode images. **(b)** Marker images. Orange and blue colors represent the inner and outer markers, respectively.

2.3 Step 3. Marker-controlled watershed transform

The marker-controlled watershed transform partitions the image by "flooding" from a predefined set of markers. Ideally, one or more of the regions initiated from the inner markers, correspond to the vessel lumen. The watershed transform is applied to the preprocessed B-mode image with respect to its corresponding marker image. The resulting image is partitioned into regions. Fig. 4a shows the result of the watershed transform applied to Fig. 2 with markers from Fig. 3b. The transform produces a set of regions that segments the image. The regions are selected if they satisfy a set of constraints, described in the next step.

2.4 Step 4. Region selection and refinement

The regions associated with the vessel lumen are selected from the segmentation result (see Fig. 4a) using two constraints. First, the regions have to contain a certain amount of flow, based on a set threshold. Second, the mean and standard deviation of the pixel intensity values inside the region should be below a set threshold. The second constraint ensures that the selected regions possess a low homogeneous intensity, as the vessel lumen. The selected regions are refined by removing pixels with very high intensity. This is followed by morphological

closing and opening. The result of this can be seen in Fig. 4b. The final segmentation is the result of a co-registration of 7 time-adjacent segmentations. The co-registration is performed by excluding pixels that are not present in at least 6 of these 7 time-adjacent segmentations. This minimizes the segmentation error, if the majority of the segmentations are correct. The selection and refinement of the regions seen in Fig. 4a results in the images seen in Fig. 4c.

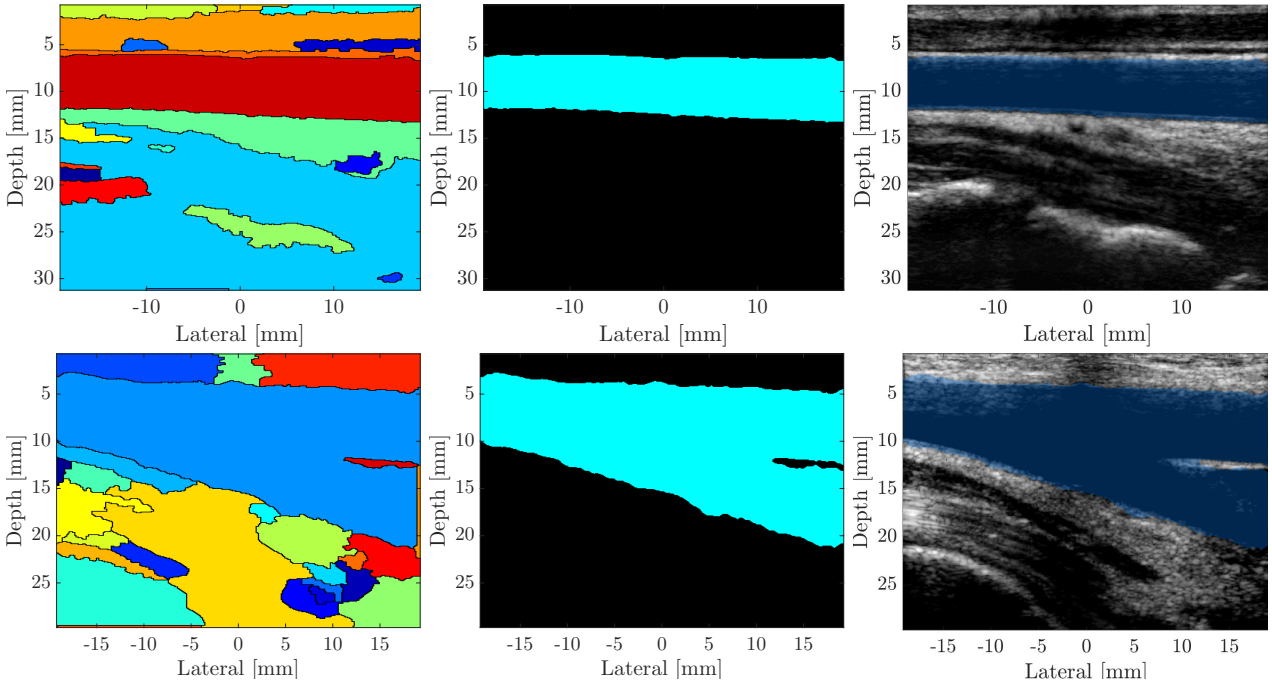

Figure 4: Example of images generated in the marker-controlled watershed transform, the region selection and region refinement. Top: CCA. Bottom: FAB. **(a)** Watershed transform applied to Fig. 2 with markers seen in Fig. 3b. **(b)** Selected and refined regions. **(c)** Final segmentation after co-registration.

3. RESULTS AND DISCUSSION

The proposed algorithm was applied to in-vivo ultrasound scans. These scans were performed on 8 healthy subjects, with 4 different vessel views. These were the CCA, CCA bifurcation, FAB, and the aorta. Each ultrasound recording included a minimum of 219 frames, from which 30 were randomly selected to be manually segmented, by two medical imaging experts. These manual segmentations served as a ground truth. This yields a complete in-vivo dataset of 1770 images. The ultrasound scans were performed by a medical doctor to achieve the correct views of the vessels. For this purpose the ultrasound system bk3000 (BK Ultrasound, Herlev, Denmark) was used as well as the two transducers "10L2w Wide Linear" and "8L2 Linear" (BK Ultrasound, Herlev, Denmark). The results are illustrated with 3 colors, where *green* refers to the manual segmentation, *blue* refers to the automatic segmentation and *red* marks the region where they overlap. The ideal segmentation, thus, yields an image with only a red color. Fig. 5 shows the result of the segmentation algorithm applied to a CCA bifurcation, FAB, and aorta along with the manual segmentation. It can be seen that there is a strong agreement, between the automatic and manual segmentations. The algorithm manages to segment all four types of vessels, demonstrating its usability in regards to different views.

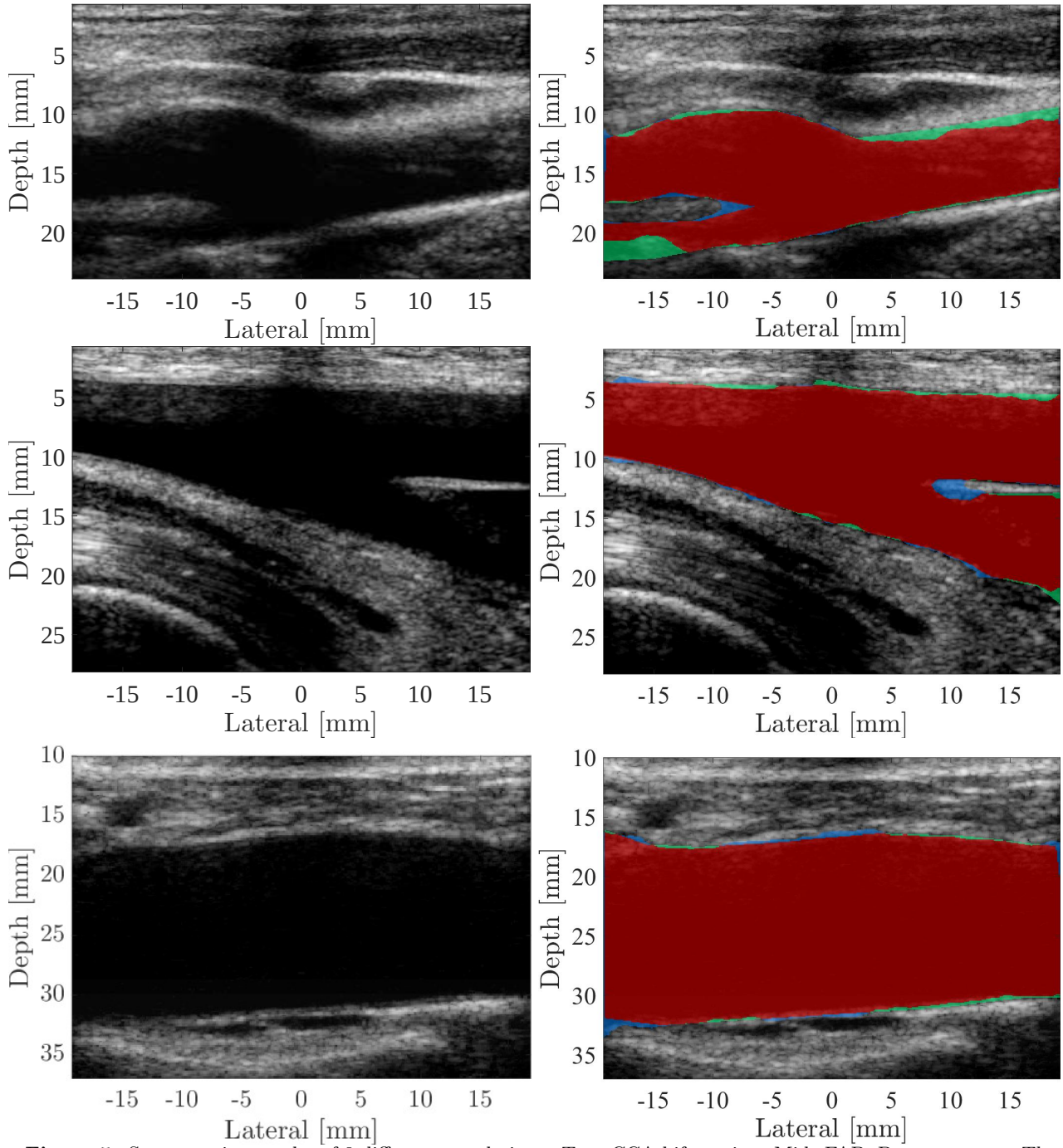

Figure 5: Segmentation results of 3 different vessel views. Top: CCA bifurcation. Mid: FAB. Bottom: aorta. The manual segmentation is marked by green, the automatic segmentation is marked by blue, and the overlap between the manual and automatic segmentation is displayed by red. The images show a strong agreement between the manual and automatic segmentation.

Evaluation of the segmentation algorithms performance was carried out, by comparing the automatic and manual segmentations using 5 different performance metrics. The metrics used to evaluate the results are the Dice similarity coefficient (DSC), sensitivity, specificity, Hausdorff distance (HD) and mean absolute distance

(MAD). The Dice similarity coefficient measures the similarity of two shapes. The coefficient ranges from 0 to 1, where 1 is a perfect agreement and 0 is no agreement. The HD indicates the worst deviation between the manual and automatic segmentation. It is calculated by finding the smallest distance between the manual and automatic segmentation for each point, with HD being the largest of these distances. The MAD is calculated as the average of smallest distances between the manual and automatic segmentation. Box plots showing the results of the segmentation algorithm in comparison to the manual segmentations can be found in Fig. 6.

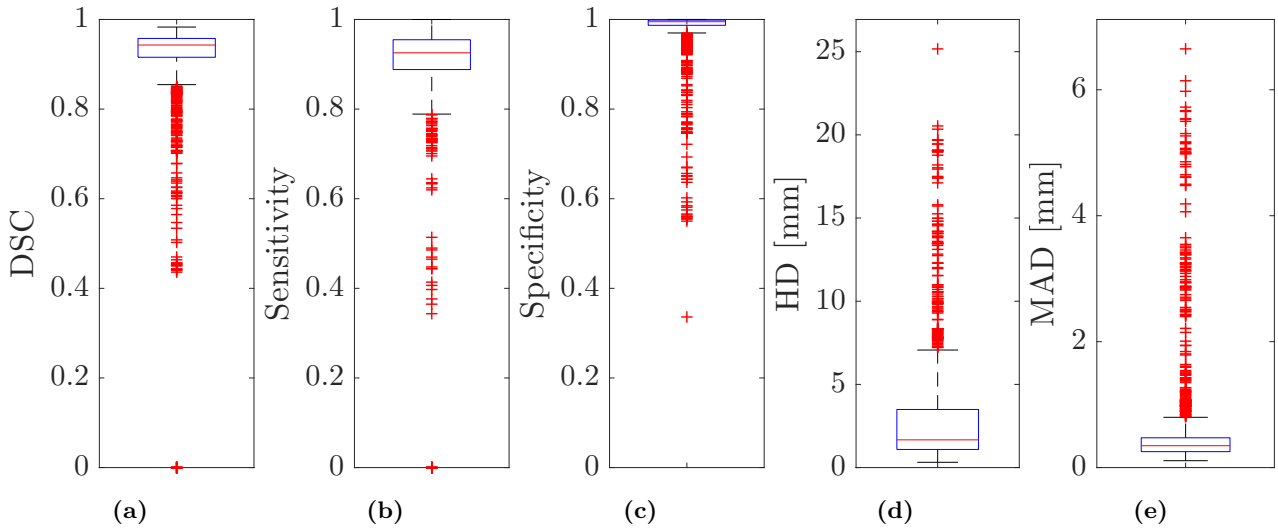

Figure 6: Box plots evaluating the performance of the proposed algorithm applied to the in-vivo dataset. The whiskers are placed at 1.5 times the interquartile range.

The box-plots of the performance metrics, indicate that there is a strong agreement between the manual and automatic segmentations performed by the proposed algorithm. Fig. 6 shows that there are occasional frames, in the form of outliers, where the segmentations are not complete. The overall performance, is summarized in Table 1, showing a sensitivity and specificity mean of above 0.9.

DSC	Sensitivity	Specificity	HD [mm]	MAD [mm]
0.9125 ± 0.116	0.9041 ± 0.112	0.9793 ± 0.057	2.98 ± 3.34	0.56 ± 0.81

Table 1: Performance metrics for the results of the in-vivo dataset (mean $\pm$ standard deviation).

3.1 Performance variation for vessel types

As seen in Fig. 7 the median of DSC is similar for each type of vessel. This suggests that the algorithms performance is consistent for the four vessel types. The median of sensitivity score is highest for segmentations of the aorta and lowest for those of the CCA, the opposite relationship is seen for the median of specificity. When segmenting the aorta, the algorithm is more prone to include parts of the neighboring tissue. The segmentations of the CCA are more susceptible to leave out parts of the vessel lumen (e.g. see Fig. 5 top). A low HD indicates a strong similarity between the shapes of the automatic segmentation and the manual segmentation. The median of HD is lowest for the segmentations of the CCA, which indicates that the false negative pixels are consistently located all around the edge of the vessel. The relatively higher median of HD score for the aorta and FAB suggests that the automatic segmentations can exclude small parts of the vessel or include a part of the tissue bordering the vessel. The median of the MAD is quite similar for all vessels types, but the interquartile range of the segmentations of the aorta is wider. In general the segmentation algorithm is robust with respect to different types of vessels.

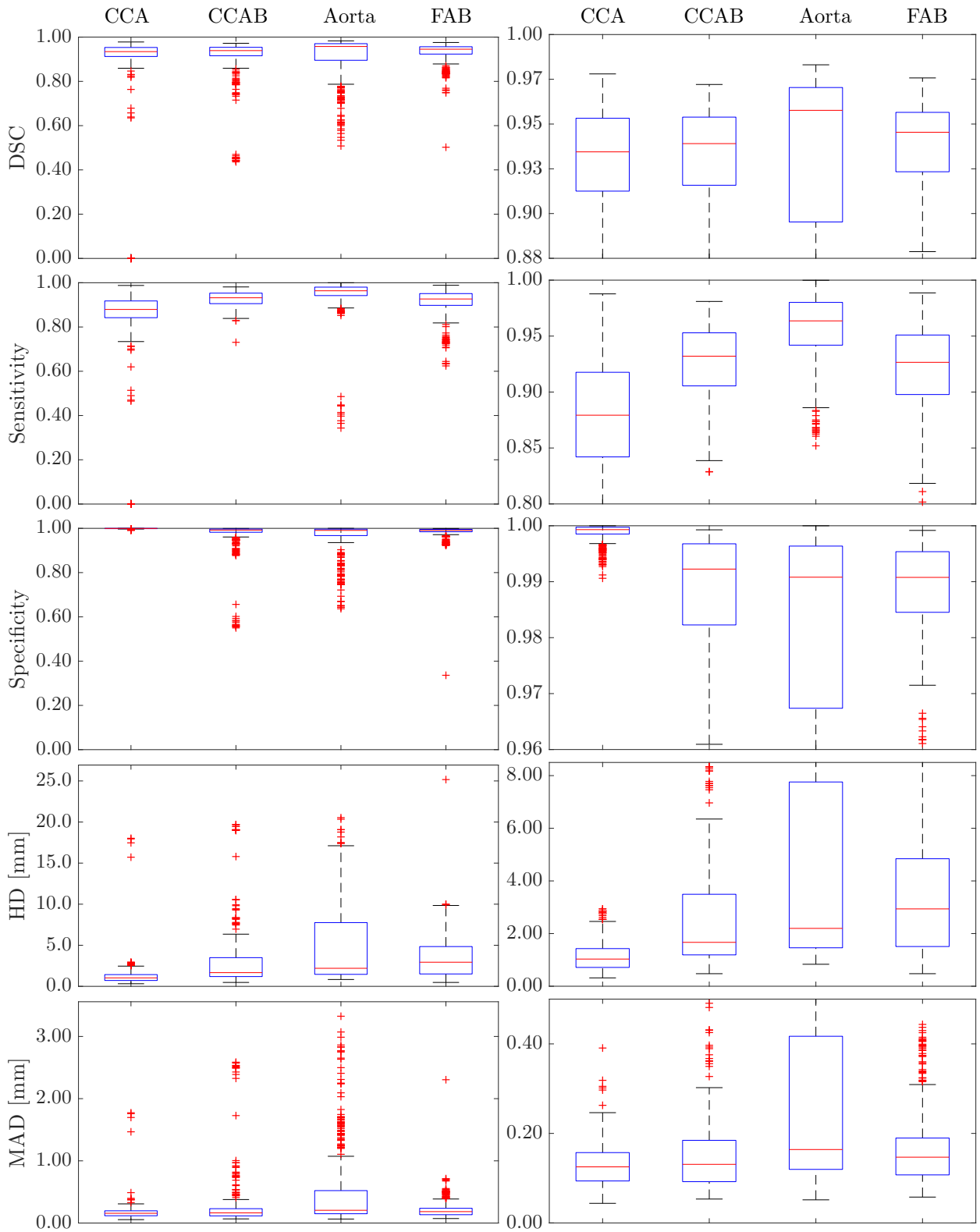

Figure 7: Performance metrics for each vessel type. The box-plots to the right are zoomed to show the variation of the interquartile range between the different vessel views. The whiskers are placed at 1.5 times the interquartile range.

3.2 Performance variation for transducers

In-vivo data was acquired from the test subjects using two different transducers. Each vessel view was scanned with both transducers. The performance metrics for both transducers are shown in Table 2. The mean values of all performance metrics are highly similar for both transducers. This supports the notion that the algorithm is also robust with respect to choice of transducer.

	DSC	Sensitivity	Specificity	HD [mm]	MAD [mm]
10L2w Wide Linear	0.9051 ± 0.139	0.8777 ± 0.146	0.9900 ± 0.018	2.76 ± 2.68	0.48 ± 0.53
8L2 Linear	0.9197 ± 0.090	0.9296 ± 0.054	0.9690 ± 0.077	3.19 ± 3.86	0.64 ± 1.00

Table 2: Performance metrics for the data obtained by the two different transducers (mean ± standard deviation).

4. CONCLUSION

An automatic algorithm for robustly segmenting the vessel lumen in ultrasound scans has been presented, using the combination of B-mode and power Doppler images. The algorithm was evaluated with respect to manual segmentations, performed by medical imaging experts. The empirical results exhibited a high level of agreement between the automatic and manual segmentation. The algorithm achieved a DSC of 91.25 ± 11.6 %, 90.41 ± 11.2 % and 97.93 ± 5.7 % (mean ± standard deviation) for the sensitivity and specificity respectively. It was shown that there is a minor variation between the different vessel views and choice of transducer. The results presented in this paper demonstrate the feasibility of automatically and robustly segmenting the vessel lumen in ultrasound images, using the marker-controlled watershed transform. The proposed algorithm can assist in quantitative feature extraction, such as the lumen diameter.

REFERENCES

[1] de Korte, C. L., Hansen, H. H. G., and van der Steen, A. F. W., "Vascular ultrasound for atherosclerosis imaging," *Interface Focus* **1**(4), 565–575 (2011).

[2] Bots, M. L., Hoes, A. W., Koudstaal, P. J., Hofman, A., and Grobbee, D. E., "Common carotid intima-media thickness and risk of stroke and myocardial infarction: The Rotterdam study," *Circulation* **96**(5), 1432–1437 (1997).

[3] Stein, J. H., Korcarz, C. E., Hurst, R. T., Lonn, E., Kendall, C. B., Mohler, E. R., Najjar, S. S., Rembold, C. M., and Post, W. S., "Use of carotid ultrasound to identify subclinical vascular disease and evaluate cardiovascular disease risk," *J. Am. Soc. Echocardiog.* **21**(2), 93–111 (2008).

[4] Beucher, S., "The watershed transformation applied to image segmentation," *Scanning Microscopy-Supplement* , 299–314 (1992).

[5] Santos, A. M. F., dos Santos, R. M., Castro, P. M. A., Azevedo, E., Sousa, L., and Tavares, J. M. R., "A novel automatic algorithm for the segmentation of the lumen of the carotid artery in ultrasound B-mode images," *Expert Systems with Applications* **40**(16), 6570 – 6579 (2013).

[6] Ramasamy, N. and B., J. K., "Automated lumen segmentation and estimation of numerical attributes of common carotid artery using longitudinal B-mode ultrasound images," in [*2013 IEEE Point-of-Care Healthcare Technologies (PHT)*], 306–309 (Jan 2013).

[7] Carvalho, D. D. B., Akkus, Z., van den Oord, S. C. H., Schinkel, A. F. L., van der Steen, A. F. W., Niessen, W. J., Bosch, J. G., and Klein, S., "Lumen segmentation and motion estimation in b-mode and contrast-enhanced ultrasound images of the carotid artery in patients with atherosclerotic plaque," **34**(4), 983–993 (2015).

[8] Lim, J. S., [*Two-Dimensional Signal and Image Processing*], Englewood Cliffs, NJ, Prentice Hall (1990).

[9] Vincent, L., "Morphological grayscale reconstruction in image analysis: applications and efficient algorithms," *IEEE Transactions on Image Processing* **2**, 176–201 (Apr 1993).

[10] Canny, J., "A computational approach to edge detection," *IEEE Transactions on pattern analysis and machine intelligence* (6), 679–698 (1986).